Conduction-band structure of graphite single crystals studied by angle-resolved inverse photoemission and target-current spectroscopy

R. Claessen, H. Carstensen, and M. Skibowski
Institut für Experimentalphysik, Universität Kiel, D-2300 Kiel, Federal Republic of Germany
(Received 26 July 1988)

We have measured the conduction-band structure of single-crystalline graphite by angle-resolved inverse photoemission spectroscopy (ARIPES) and target-current spectroscopy (TCS) up to 38.5 eV above the Fermi level. As opposed to azimuthally disordered pyrolytic graphite we find distinct differences in the ARIPES spectra between the ΓAHK and ΓALM planes of the Brillouin zone regarding intensity and energy location of the observed structures. Such differences are much less pronounced in the TCS spectra. The interpretation of a state at the Γ point near 5 eV above E_F is discussed in terms of an image-potential state or a bulk-band-derived surface state. The experimental band structure is compared with recent band-structure calculations.

I. INTRODUCTION

The electronic structure of graphite as a typical example for a layered material has been studied intensively in the past few years.[1–20] So far the following picture of the band structure has emerged: The valence band consists of σ bands derived from hybridized $2s, 2p_x, 2p_y$ atomic orbitals constituting the strong intralayer bonding and of $2p_z$-derived π bands at lower binding energies responsible for the weak van der Waals bonding between the layers. The conduction band consists of the respective antibonding σ^* and π^* bands. The full band structure is characterized by large dispersion parallel to the layers and by strong localization perpendicular to them. Thus graphite can be considered as a prototype of a two-dimensional solid. However, recent band structure calculations[1,2,6,7] going beyond a basis of only $2s$ and $2p$ orbitals yielded a σ^* state as the lowest conduction band at Γ, which has a considerable charge density between the layers (interlayer state).

While the valence-band structure has been established experimentally by angle-resolved photoemission spectroscopy[8–13] (ARPES) in good agreement with theoretical work,[1–7] the structure of the unoccupied states is still a matter of discussion both theoretically and experimentally. In particular, recent band-structure calculations of Tatar and Rabii[1] (TR) and of Holzwarth, Louie and Rabii[2] (HLR) differ considerably in their prediction concerning energy and dispersion of the interlayer state. Experimental work on the conduction bands has been done by means of secondary-electron-emission spectroscopy (SEES),[5,9,10,11,13] constant-final-state spectroscopy (CFS),[14] electron-energy-loss spectroscopy (EELS),[15] angle-resolved inverse photoemission spectroscopy (ARIPES),[16–19] and target-current spectroscopy (TCS).[18,20] As far as the low-lying conduction bands are concerned, the angle-resolved SEES and CFS data are not consistent with those obtained by ARIPES and TCS.

All previous ARIPES studies were done on highly oriented pyrolytic graphite (HOPG), i.e., rotationally disordered samples. Here we present a detailed mapping of the conduction band structure of *single-crystalline graphite* obtained by ARIPES up to 25 eV above the Fermi level. These measurements are supplemented by angle-resolved target-current spectroscopy (up to 38.5 eV above E_F).

II. EXPERIMENTAL DETAILS

ARIPES is a rapidly developing technique for wave-vector-resolved determination of the unoccupied electronic states.[21–24] In ARIPES a collimated electron beam of well-defined energy impinges on the surface of the sample under a known angle of incidence. The photon flux generated by radiative transitions of the incoming electrons into unoccupied states in the sample is measured. From the conservation of the surface component of the wave vector $k_\parallel$, the detected photon energy $h\nu$, the kinetic energy, and the angle of incidence ϑ of the electrons, a two-dimensional experimental band structure $E(k_\parallel)$ can be derived similar to the procedure in ARPES.

In TCS the current absorbed by the sample is measured as a function of the kinetic energy of the impinging electron beam. The modulation in the current is attributed mainly to elastic electron scattering.[18,25–28] High reflectivity corresponding to a minimum in the target current is expected if the electron energy falls into a gap of the band structure or if the symmetry of the states in the solid does not allow matching to the incoming plane wave at the surface. Enhanced current is expected at energies where the incoming electrons can couple into Bloch states in the crystal. As discussed in a previous paper[18] this interpretation differs from other work in which inelastic processes are considered important.[20,28]

Details of the ARIPES spectrometer have been published elsewhere.[29,30] The low-energy-electron source has an energy resolution of 220 meV (FWHM) and a wave vector resolution of ≈ 0.08 Å^{-1}. The bandpass photon detector consisting of an open Cu-Be multiplier with a KBr photocathode and a CaF_2 entrance window operates

at a photon energy of 9.9 eV. The energy resolution of the detector is 600 meV (FWHM), which is known from its spectral sensitivity measured with synchrotron radiation. Thus it is possible to deconvolute the ARIPES spectra with the known spectrometer function in order to obtain an enhanced resolution. The same electron gun was used in both ARIPES and TCS. The experimentally determined Fermi level of a sputtered Au film was used as an energy reference in these measurements.

The sample was cut from a natural graphite single crystal (originating from Baffin Island, Canada). The high-symmetry directions were determined by x-ray diffraction and low-energy electron diffraction (LEED). Azimuthal misalignment was estimated to be less than 5°. The sample was cleaved *in situ* at a base pressure in the low 10^{-10} Torr range. The work function was determined from the onset of the target current of a negative biased sample (≈ 10 V) in normal incidence to be 4.7 eV in close agreement with other work.

III. RESULTS AND DISCUSSION

A. Inverse photoemission

ARIPES spectra of the graphite single crystal were taken in the two high-symmetry planes ΓALM and ΓAHK, going from normal electron incidence ($\vartheta = 0°$) to $\vartheta = 85°$ by increments of 2.5°. A selection of spectra is shown in Fig. 1. The spectra show remarkable modulation up to 25 eV above the Fermi level. They also reveal distinct differences between the two directions. The observed peaks and their dispersion are labeled by capital letters $A-N$. A detailed evaluation of the spectra and a comparison to the band-structure calculations of TR (Ref. 1) and HLR (Ref. 2) is shown in Figs. 2 and 3.

The most prominent structure in both series of spectra is peak A with a strong upward dispersion from high to low angles of incidence which is attributed to the low-lying antibonding π^* bands. We find marked differences for the intensity of this peak between ΓAHK and ΓALM. In particular, in the ΓALM plane there is a remarkable decrease of intensity for $\vartheta < 70°$ accompanied by an asymmetric line shape. Deconvolution of ΓALM spectra shows that this shape can be resolved into two peaks lying approximately 1 eV apart, which is in close agreement with the π^* band splitting as predicted by HLR.

All spectra show a nondispersing feature (B) at 1.8 eV as seen in all previous ARIPES studies on HOPG.[16–19] It has been attributed to indirect transitions into the high density of states (DOS) of the π^* band at the M point. From our measured dispersion of this π^* band we estimate a value of 2.5 eV above E_F at M. This difference may be understood by $k_\perp$ effects expected from the theoretically predicted $k_\perp$ dispersion of this band of approximately 0.7 eV along the ML line.[1] A different explanation for a similar nondispersing feature observed in ARPES (Ref. 8) uses emission from isolated carbon atoms sitting on top of the outermost layer of the crystal, but we did not observe any dependence on contamination or aging.

Peak C at 3.7 eV in normal incidence, having both width and shape of the spectrometer function, shows an upward dispersion away from Γ in both directions, followed by a strong intensity variation and a slight downward dispersion when coming close to peak A (π^* band). For HOPG the same behavior is indicated in the ARIPES spectra of Schäfer *et al.*,[18] while no deviation from a parabolic dispersion has been observed in Ref. 19. From photon-energy-dependent[16] ARIPES on HOPG this state is known to have no dispersion normal to the layers. Schäfer *et al.* also observed a decrease of intensity after a strong accidental contamination of their sample. Thus it has to be attributed to a surface state in contradiction to Ref. 17. Posternak *et al.*[7] found from thin-film calculation on graphite an unoccupied surface state at 3.8 eV derived from the volume $\sigma^*(\Gamma_1^+)$ band (interlayer state). An alternative explanation for the surface state has been proposed by Schäfer *et al.*; due to the absence of crystal states near the vacuum level around the Γ point an incident electron may be bound by its own image charge, thus constituting a Rydberg-like series of image potential states[21] with a maximum binding energy of 0.85 eV (for $n = 1$) with respect to the vacuum energy. Taking the measured value of 4.7 eV for the work function, this results in an energy of 3.85 eV above E_F close

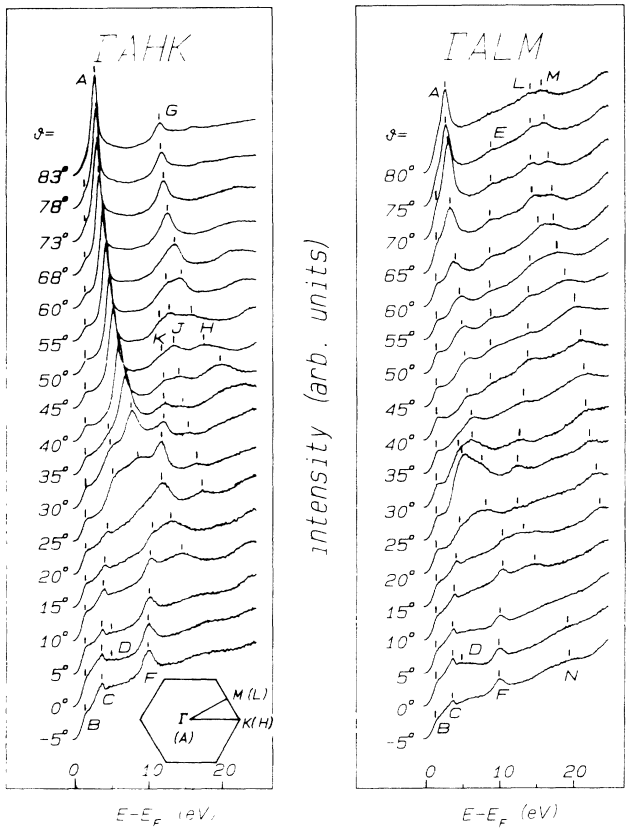

FIG. 1. Inverse photoemission spectra up to 25 eV above the Fermi level E_F in the two high symmetry planes ΓAHK and ΓALM for various angles of electron incidence. The features labeled $A-N$ are discussed in the text. Inset showing the basal plane of the graphite Brillouin zone.

to the observed value. However, with most of its charge density far in the vacuum, an image-potential state should be very sensitive to strong electric fields as they occur in scanning tunneling microscopy (STM) resulting in a Stark shift of its energy position. Such behavior in STM spectra has been observed for the image state of the Ni(100) surface.[31] A STM spectrum of graphite (HOPG) published by Reihl *et al.*[17] shows a state at 3.3 eV above E_F, which the authors associate with the 3.5 eV state observed in photon-energy-dependent ARIPES.[16,32] This seems to indicate the absence of a Stark shift, though the STM spectrum is only taken up to 4 eV. Therefore STM spectroscopy of graphite over a wider energy range is necessary in order to clarify the interpretation of the observed surface state. The effective masses of this state near Γ obtained from a parabolic fit of the dispersion along ΓM and ΓK are $(1.2\pm0.2)m_0$ and $(1.5\pm0.2)m_0$, respectively. Previous work on HOPG gives $1.3m_0$ (Ref. 18) and $1.2m_0$ (Ref. 19) as azimuthally averaged values.

For the spectra taken in or near normal incidence we observe a faint emission around 5 eV, denoted by *D*. This structure has been seen before in ARIPES on HOPG with both fixed[18] and variable[16] photon energy. In the latter study it has been shown to possess a considerable $k_\perp$ dispersion in concordance with the theoretical $\sigma^*(\Gamma_1^+)$ band of HLR. The low intensity can be explained from the 3*s* orbital character of this state, since it is known from photoemission[33] that the cross section for transitions into *s*-like states is much smaller than for *p*-like states at the photon energy used here (9.9 eV). Band-structure calculations[1,2] predict a strong upward dispersion of this band along ΓK but a considerably reduced dispersion along ΓM with a high DOS at *M* (cf. Figs. 2 and 3). We observe a structure at 8.8 eV in the ΓALM spectra denoted by *E*, which also occurs in spectra of HOPG samples.[18,19] As it has been already suspected there this peak can clearly be attributed to the $\sigma^*(M_1^+, M_2^-)$ states since we observe no counterpart in the ΓAHK spectra. When following structure *E* to higher angles of incidence one crosses the Brillouin zone (BZ) boundary at $\vartheta = 50°$. Thus this peak is most pronounced for values of $k_\parallel$ in the second BZ.

In both series of spectra a distinct feature (*F*) near normal incidence at 10.0 eV occurs which lies close to the previously observed values of 9.7,[18] 9.0,[19] and 9.5 eV.[16] The last authors found a vanishing $k_\perp$ dispersion and therefore ascribed this peak to the $\sigma^*(\Gamma_5^+, \Gamma_6^-)$ bands. Here is the place to comment on the controversial results for the low-lying σ^* bands obtained by the different spectroscopic methods as mentioned above. Spectra of photon-excited[9,11,13] or electron-excited[5,34] secondary-electron-emission spectroscopy show a feature at 7.5 eV, in contradiction to inverse photoemission studies,[16–19] including this work, where this structure has not been observed. This may be due to the different kinds of processes involved in the two spectroscopies. In inverse photo-

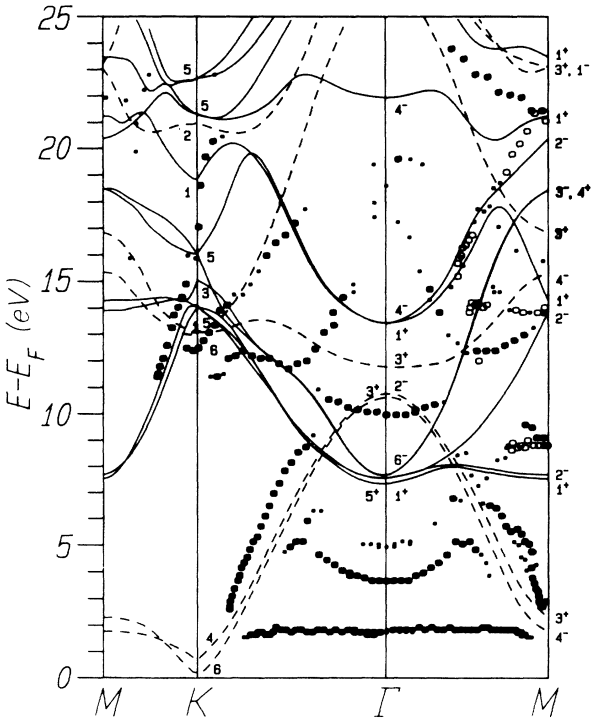

FIG. 2. Comparison of the experimental data (circles) obtained by ARIPES with the calculation of Tatar and Rabii (Ref. 1), π^* bands (dashed lines), σ^* bands (solid lines). The theoretical bands are labeled by their irreducible representations at the critical points. Small circles denote weak structures or shoulders in the original spectra, open symbols denote states obtained by folding back into the first Brillouin zone.

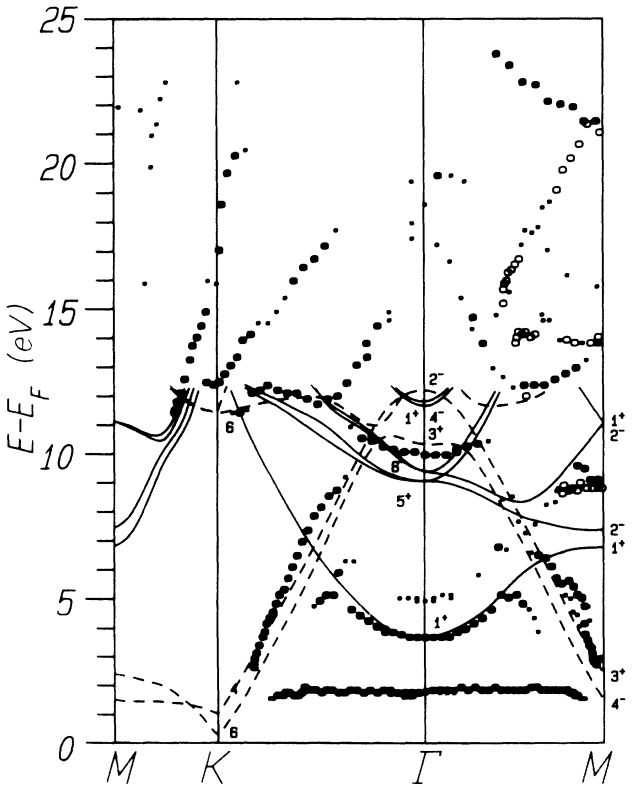

FIG. 3. Experimental data as in Fig. 2, but compared with the calculation of Holzwarth *et al.* using the Hedin-Lundqvist exchange correlation (Ref. 2).

emission an initially free electron makes an optical transition to a crystal state, which is supported by a high one-dimensional density of final states normal to the surface. Thus we observe a distinct emission associated with the $\sigma^*(\Gamma_5^+,\Gamma_6^-)$ band, which from calculations[1,2] is known to have no dispersion along ΓA resulting in a high DOS in the projected band structure. Similarly, we are able to detect the $\sigma^*(\Gamma_1^+)$ state at 5 eV due to its vanishing $k_\perp$ dispersion near the Γ point, though the small matrix element for the transition reduces its intensity dramatically. On the other hand, the high group velocity of this band perpendicular to the surface around the A point may support transport of electrons in this state through the surface, as this is required in SEES.[11] Theoretical values for the energy of the $\sigma^*(A_1)$ state are 6.5 (Ref. 2) and 9.0 eV (Ref. 1). This is in reasonable agreement with the observed structure at 7.5 eV in SEES. Thus this state could be attributed to the $\sigma^*(A_1)$ state. The assignment of Ref. 13 as a $\sigma^*(\Gamma_5^+)$ state must be wrong, since this band has not the required symmetry Δ_1 or Δ_2 to be matched to a plane wave at normal emission.[12]

In the ΓAHK plane a pronounced feature (G) occurs at 11 eV for $\vartheta=83°$. Due to the high angle of incidence this state is already outside the first BZ and disperses up to 15 eV along the MK (LH) direction when going to lower angles. Comparison with the calculations of TR and HLR (Figs. 2 and 3) clearly shows that this structure has to be attributed to the $\sigma^*(K_{1,5},M_1^+,M_2^-)$ band, which is a branch of the interlayer state. Unfortunately, the photon energy used in this experiment (9.9 eV) did not allow us to follow this state through to the critical point M in order to verify the energy of this state measured in the ΓALM direction. Going to even lower angles the BZ boundary (KH line) is crossed at $\vartheta=55°$, where structure G splits into three peaks H, J, and K. Feature H rises strongly in energy while broadening considerably. By comparison to theory it can hardly be ascribed to a single band but rather it has to be attributed to various parts of high DOS at the critical line KH. Peak J disperses from 12.4 eV at K (H) to 18 eV halfway of the ΓAHK plane following closely the theoretical $\pi^*(\Gamma_2^-,K_6)$ band of TR. Starting at the KH edge of the BZ, peak K seems to follow at least qualitatively the calculated dispersion of the $\pi^*(\Gamma_3^+,K_6)$ band, but then shows a strong dispersion from 11.5 eV up to 17–18 eV at the center of the BZ while the intensity strongly decreases. A similar structure (denoted by L) with an almost symmetric dispersion can be seen in the ΓALM spectra. These structures have also been observed in Refs. 18 and 19. They are somewhat puzzling since they have no counterparts in the high-energy band-structure calculations.[1,5] The highest π^* band in the calculation of HLR seems to indicate a qualitatively similar dispersion though over a much smaller energy range. Structure L crosses the M point for $\vartheta=40°$ at an energy of 13.8 eV. For higher angles it shows almost no dispersion. From folding back this band into the first BZ we obtain a flat band from M to about $\frac{1}{2}\Gamma M$, which cannot be explained by the calculation of TR (Fig. 2).

Finally, we have peak M in the ΓALM plane dispersing down from 24 eV at $\vartheta=20°$ to 15 eV at $\vartheta=80°$. When crossing the BZ boundary ($\vartheta=35°$) the slope of the dispersion abruptly changes. Figure 2 shows that peak M belongs to two different bands, one dispersing down from high energies near Γ to 21.5 eV at the critical point M only seen in the first BZ, while the band lower in energy disperses upwards from the center of the BZ to the M point, and is observed only in the second BZ (in Figs. 2 and 3 it has been folded back into the first BZ). We ascribe the low-energy band to the $\sigma^*(\Gamma_4^-,M_2^-)$ band of the calculation of TR. One might be tempted to attribute the high-energy part of structure M to the $\sigma^*(\Gamma_4^-,M_1^+)$ band, but we know from Refs. 18 and 19 that this band lies lower in energy at about 19–20 eV near Γ, which is confirmed by the weak emission N in our ARIPES spectra and by our TCS results (see Sec. III B). Rather, we interpret structure M for $\vartheta>35°$ as belonging to the $\sigma^*(\Gamma_1^+,M_1^+)$ band of TR, which has the same dispersion as the observed state. Thus the splitting of the σ^* bands on the ML line around 22 eV seems to be smaller than theoretically predicted.

From the behavior of the structures M and L, and, to a lesser extent, E, we see that some bands can only be detected if the wave vector $\mathbf{k}$ of the incident electron lies within the first BZ, while for other bands one has to go into the second BZ. Similar effects have been observed in ARPES measurements of single-crystalline graphite[11] and other materials,[35] where sharp intensity changes occur as certain bands cross zone boundaries. Such intensity asymmetries can be explained by detailed consideration of the symmetry of the crystal-state wave functions and their matching at the surface to the plane waves in vacuum.[12] The fact that graphite has a nonsymmorphic space group (C_{6v}^4) may be here of some importance as this was shown to be the case for photoelectron emission normal to the (0001) surface.[11,12]

B. Target-current spectroscopy

We now turn to the results obtained by TCS. We measured the sample current for incident electron energies of 8.5–38.5 eV above the Fermi level, while the angle of incidence varied from 0° to 70°. Except for the measurement of the work function all TCS data were taken under field-free conditions. The spectra are shown in Fig. 4. Though we were not able to reproduce the astonishingly strong current modulation observed by Schäfer *et al.*[18] there is still significant structure in the spectra, the location of which agrees well with the HOPG results. In order to enhance the information of the data and to get rid of a linearly rising background we evaluated the maxima of the negative second derivative of the spectra. Only structure also visible in the original data was taken into account. The result is an experimental band structure shown in Fig. 5 in comparison to the calculation of TR. We will discuss now only the important features.

There is a band dispersing from 10 eV above E_F at Γ to ≈ 12 eV when going towards both critical points M and K. It is almost 2 eV lower in energy than the $\pi^*(\Gamma_3^+)$ band of TR, while having the same dispersion. A somewhat better agreement is obtained by comparison with the π^* bands around 11 eV in the HLR calculation. Al-

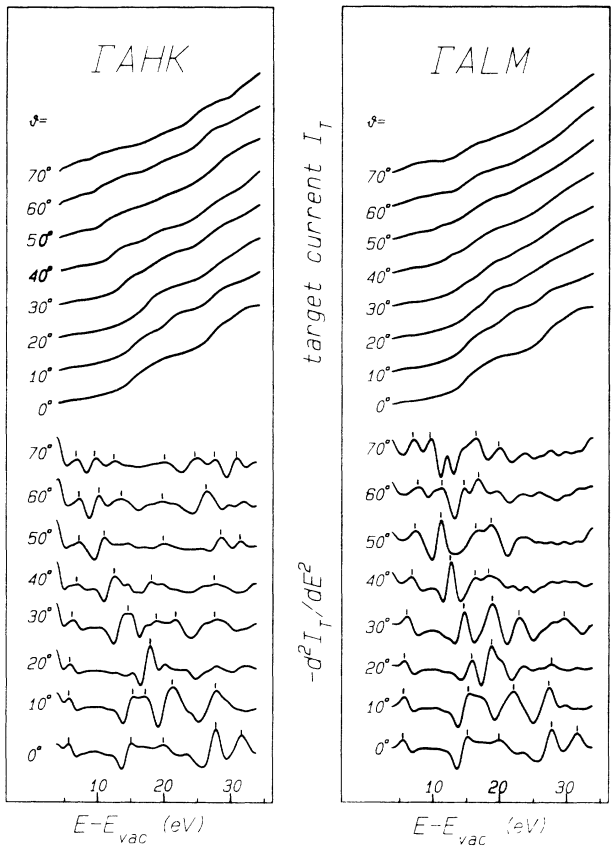

FIG. 4. Upper half showing the current I_T absorbed by the sample for electrons incident under various angles in the ΓAHK and ΓALM planes as a function of kinetic energy. Lower half, the respective negative second derivatives of the TCS spectra. Tick marks indicate structure attributed to coupling into conduction band states.

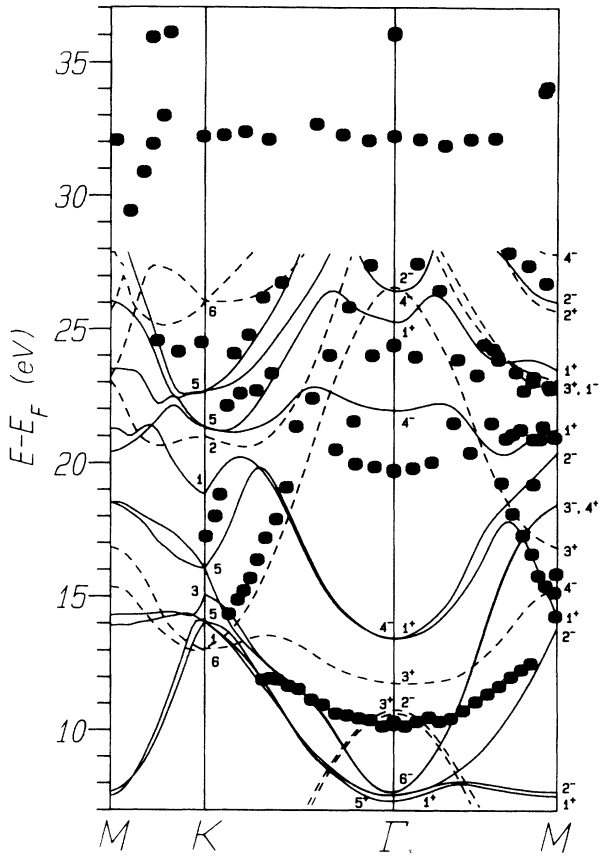

FIG. 5. Comparison of the TCS data with the calculation of Tatar and Rabii (Ref. 1) in the energy range from 7–37 eV above the Fermi level.

though we ascribed the emission F at 10.0 eV measured in ARIPES to the $\sigma^*(\Gamma_5^+,\Gamma_6^-)$ states, the TCS structure at 10 eV must be interpreted as due to the $\pi^*(\Gamma_3^+)$ state, because only this state has the correct Δ_1 symmetry to be matched to a plane wave at normal incidence. A structure dispersing from 14 eV near K to higher energies can up to 19 eV be ascribed to the $\pi^*(\Gamma_2^-,K_6)$ band. We observed this band also in ARIPES though about 1 eV lower in energy. Following the TCS peak to even higher energies up to 28 eV above the Fermi level it rather resembles the still higher-lying π^* band of TR. A similar feature occurs in the ΓALM spectra, possibly also reflecting the high-lying π^* bands, although the measured energy at M is 15 eV, as opposed to 17 eV in the calculation. The TCS data also reveal a band around Γ with an energy of 20 eV slightly dispersing up to 21 eV at M, which has to be ascribed to the $\sigma^*(\Gamma_4^-)$ band already observed in ARIPES as the weak emission N. A structure near the M point at 23 eV with a moderate upward dispersion when going towards the center of the BZ is probably due to the π^* band with M_1^- symmetry, since this band has the highest group velocity normal to the surface of all bands in that region of **k** space.

The TCS results are in very good agreement with those of Schäfer *et al.* obtained on azimuthally disordered pyrolytic graphite. The spectra of the single crystals show with few exceptions only weak dependence on the direction measured, as opposed to the ARIPES data. At the high energies used in TCS the effect of crystal potential on the band structure is only small, as the calculations[1,5] show. The only symmetry dependence arises from the matching of the incident plane wave to the crystal state. In ARIPES one has the *additional* process of an optical transition into the final state, which is stronger affected by the crystal potential. This process involves *two* crystal wave functions (and the direction of the optical **E** field), so the matrix element describing this transition significantly depends on crystal direction. Therefore the ARIPES intensities have a marked asymmetry between the different directions probed in momentum space, while TCS spectra show only slight dependence.

C. Comparison with band-structure calculations

In this section we briefly summarize the comparison of the experimental band structure determined by ARIPES with the calculations of Tatar and Rabii (Fig. 2) and

TABLE I. Critical-point energies in eV above E_F.

	Experimental		Band-structure calculations		
	ARIPES	TCS	TR (Ref. 1)	HLR (Ref. 2)	Ref. 7
Γ-point states					
surface state	3.7				3.8
$\sigma^*(\Gamma_1^+)$	4.9[a]		7.1	3.7	4.2
$\sigma^*(\Gamma_5^+,\Gamma_6^-)$	10.0		7.3/7.3	9.0/9.3	
$\pi^*(\Gamma_3^+)$		10.3	11.7	10.4	
$\pi^*(?)$	$\sim$17–18				
$\sigma^*(\Gamma_4^-)$	19.6	19.7	22.0		
K-point states					
$\pi^*(K_6)$	12.4	<14[b]	13.0	11.4	
$\sigma^*(K_{1,6})$	>15[b]		14.0	>12.5	
M-point states					
$\pi^*(M_3^+,M_4^-)$	1.8[c]/$\sim$2.5[b]		1.8/2.6	1.5/2.4	
$\sigma^*(M_1^+,M_2^-)$	8.8		7.4/7.5	6.7/7.4	
$\pi^*(M_4^-)$	13.8		15.2		
$\pi^*(M_3^+)$		$\sim$15	15.8		
$\sigma^*(M_2^-)$	21		20.3		
$\sigma^*(M_1^+)$		21	21.1		
$\sigma^*(M_1^+)$	21		23.5		
$\pi^*(M_1^-)$		23	23.0		

[a] $k_\perp$ effects not considered (see text).
[b] From extrapolation of observed dispersion.
[c] From nondispersing feature B.

Holzwarth *et al.* using the Hedin-Lundquist exchange correlation (Fig. 3). Figure 5 shows the TCS data compared to the high-energy range of the TR calculation. Though we have no information on the component of the wave vector normal to the surface ($k_\perp$) in the experimental data we are able to compare with the theoretical bands in the ΓKM plane because only few bands show a marked dependence on $k_\perp$.

The overall agreement of experimental and theoretical energies is satisfactory regarding the difficulties in calculating precise conduction band structures. In the low-energy range from 0–12 eV above E_F we find good agreement with the calculation of HLR. The π^* bands and the $\sigma^*(\Gamma_5^+,\Gamma_6^-)$ states are reproduced within 1 eV, the $\sigma^*(\Gamma_1^+)$ state is found to be 1.3 eV higher in energy than in theory. Neither of the calculations is able to predict correctly the energy of the interlayer state at the M point. The comparison of our data to the work of TR shows major discrepancies for the low-lying σ^* bands, but considering the lack of self-consistency in this calculation and the large energy range covered we find excellent agreement for some of the bands between 10 and 25 eV [$\sigma^*(K_{1,5},M_1^+,M_2^-),\pi^*(\Gamma_2^-,K_6),\sigma^*(\Gamma_4^-,M_2^-)$]. We cannot confirm the existence of a large energy gap around the Brillouin-zone center from 14–22 eV as it is predicted by TR and similarly in Ref. 5. Rather, we find the $\sigma^*(\Gamma_4^-)$ state much lower in energy at 19.5 eV in ARIPES (20 eV in TCS) and a strongly dispersing band with its top at 17–18 eV at Γ possibly having π^* character, which has no theoretical explanation as yet. Table I shows the critical point energies measured in this work in comparison to the calculated values of Refs. 1, 2, and 7.

IV. CONCLUSION

We have measured the unoccupied electronic structure of single-crystalline graphite over an energy range from 0–25 eV above the Fermi level by means of combined angle-resolved inverse photoemission and target-current spectroscopy. We observed marked differences between the measured high-symmetry planes ΓAHK and ΓALM in ARIPES, but much less pronounced in TCS. Comparison to band-structure calculations gives good agreement with that of Holzwarth *et al.* for bands below 12 eV. For energies above 12 eV there is partial agreement with the work of Tatar and Rabii, but we also find discrepancies for bands in the center region of the Brillouin zone. Here a refined calculation of the high-lying conduction bands is needed to explain the data of the inverse photoemission studies. A surface state at 3.7 eV above E_F shows slightly different dispersions along the ΓK and ΓM direction. The question of whether to interpret this state as an $n=1$ image potential state or as a volume-band-derived surface state cannot be decided by inverse photoemission at present. Further investigation of this state by scanning tunneling spectroscopy could help to clarify the situation, since an image potential state should show a detectable Stark shift.

ACKNOWLEDGMENTS

We thank G. Brusdeylins and C. Heimlich (both at the Max-Planck-Institut für Strömungsforschung, Göttingen) for kindly supplying us the natural graphite crystals. This work was supported by the Deutsche Forschungsgemeinschaft (Bonn, Germany).

[1]R. C. Tatar and S. Rabii, Phys. Rev. B **25**, 4126 (1982).
[2]N. A. W. Holzwarth, S. G. Louie, and S. Rabii, Phys. Rev. B **26**, 5382 (1982).
[3]C. P. Mallet, J. Phys. C **14**, L213 (1981).
[4]A. Zunger, Phys. Rev. B **17**, 626 (1978).
[5]R. F. Willis, B. Fitton, and G. S. Painter, Phys. Rev. B **9**, 1926 (1974).
[6]M. Posternak, A. Baldereschi, A. J. Freeman, E. Wimmer, and M. Weinert, Phys. Rev. Lett. **50**, 761 (1983).
[7]M. Posternak, A. Baldereschi, A. J. Freeman, and E. Wimmer, Phys. Rev. Lett. **52**, 863 (1984).
[8]I. T. McGovern, W. Eberhardt, E. W. Plummer, and J. E. Fischer, Physica B **99**, 415 (1980).
[9]A. R. Law, J. J. Barry, and H. P. Hughes, Phys. Rev. B **28**, 5332 (1983).
[10]D. Marchand, C. Frétigny, M. Laguës, F. Batallan, Ch. Simon, I. Rosenman, and R. Pinchaux, Phys. Rev. B **30**, 4788 (1984).
[11]A. R. Law, M. T. Johnson, and H. P. Hughes, Phys. Rev. B **34**, 4289 (1986).
[12]D. Pescia, A. R. Law, M. T. Johnson, and H. P. Hughes, Solid State Commun. **56**, 809 (1985).
[13]T. Takahashi, H. Tokailin, and T. Sagawa, Phys. Rev. B **32**, 8317 (1985).
[14]A. R. Law, M. T. Johnson, H. P. Hughes, and H. A. Padmore, J. Phys. C **18**, L297 (1985); M. T. Johnson, A. R. Law, and H. P. Hughes, Surf. Sci. **162**, 11 (1985).
[15]L. Papagno and L. S. Caputi, Surf. Sci. **125**, 530 (1983).
[16]Th. Fauster, F. J. Himpsel, J. E. Fischer, and E. W. Plummer, Phys. Rev. Lett. **51**, 430 (1983).
[17]B. Reihl, J. K. Gimzewski, J. M. Nicholls, and E. Tosatti, Phys. Rev. B **33**, 5770 (1986).
[18]I. Schäfer, M. Schlüter, and M. Skibowski, Phys. Rev. B **35**, 7663 (1987).
[19]H. Ohsawa, T. Takahashi, T. Kinoshita, Y. Enta, H. Ishii, and T. Sagawa, Solid State Commun. **61**, 347 (1987); F. Maeda, T. Takahashi, H. Ohsawa, and S. Suzuki, Phys. Rev. B **37**, 4482 (1988).
[20]A. Dittmar-Wituski, M. Naparty, and J. Skonieczny, J. Phys. C **18**, 2563 (1985).
[21]D. Straub and F. J. Himpsel, Phys. Rev. B **33**, 2256 (1986).
[22]V. Dose, Prog. Surf. Sci. **13**, 225 (1983).
[23]N. V. Smith, Vacuum **33**, 803 (1983).
[24]J. B. Pendry, J. Phys. C **14**, 1381 (1981).
[25]E. G. McRae, J. M. Landwehr, and C. W. Caldwell, Phys. Rev. Lett. **38**, 1422 (1977).
[26]R. C. Jaklevic and L. C. Davis, Phys. Rev. B **26**, 5391 (1982).
[27]E. Tamura, R. Feder, and J. Krewer, Solid State Commun. **55**, 543 (1985).
[28]L. T. Chadderton and S. A. Komolov, Surf. Sci. **90**, 359 (1979).
[29]N. Babbe, W. Drube, I. Schäfer, and M. Skibowski, J. Phys. E **18**, 158 (1985).
[30]I. Schäfer, W. Drube, M. Schlüter, G. Plagemann, and M. Skibowski, Rev. Sci. Instrum. **58**, 710 (1987).
[31]G. Binnig, K. H. Frank, H. Fuchs, N. Garcia, B. Reihl, H. Rohrer, F. Salvan, and A. R. Williams, Phys. Rev. Lett. **55**, 991 (1985).
[32]While Fauster *et al.* (Ref. 16) assign their state to a possible surface state, Reihl *et al.* (Ref. 17) rule out this possibility from their adsorbate experiments. Schäfer *et al.* (Ref. 18) argued that the amount of exposure used by Reihl *et al.* (33 L O_2^* or 150 L H_2^*) seems far too low to quench an image-potential state.
[33]A. Bianconi, S. B. M. Hagström, and R. Z. Bachrach, Phys. Rev. B **16**, 5543 (1977).
[34]R. F. Willis, B. Feuerbacher, and B. Fitton, Phys. Lett. **34A**, 231 (1971).
[35]E. Dietz and D. E. Eastman, Phys. Rev. Lett. **41**, 1674 (1978).